



MINISTRY OF AVIATION

AERONAUTICAL RESEARCH COUNCIL

CURRENT PAPERS

Experiments at Hypersonic Speeds on Circular Cones at Incidence

By

DH. Peckham

LONDON: HER MAJESTY'S STATIONERY OFFICE

1965

SIX SHILLINGS NET

U.D.C. No. 533.696.4 : 533.6.048.2 : 533.6.011.55

C.P. No. 702

January, 1963

EXPERIMENTS AT HYPERSONIC SPEEDS ON
CIRCULAR CONES AT INCIDENCE

by

D.H. Peckham

SUMMARY

Pressure distribution measurements on five circular cones with total apex-angles ranging from 25 to 45 degrees are described. The tests covered a range of angles of incidence from 0 to 30 degrees, at Mach numbers of 6.85 and 8.60. The extent to which various analytical and empirical theories predict the measured pressures is assessed.

LIST OF CONTENTS

	<u>Page</u>
1 INTRODUCTION	4
2 DESCRIPTION OF TESTS	4
3 METHODS OF CALCULATING INVISCID SURFACE PRESSURE DISTRIBUTIONS	5
3.1 General	5
3.2 The M.I.T. tables	5
3.3 Shock-layer theories	6
3.4 Empirical methods	8
4 COMPARISON OF RESULTS WITH AVAILABLE METHODS FOR CALCULATING PRESSURE DISTRIBUTIONS	9
4.1 Cones at zero incidence	9
4.2 Cones at incidence	10
4.2.1 Comparison with the M.I.T. tables	10
4.2.2 Comparison with the shock-layer theories	11
4.2.3 Comparison with empirical theories	12
5 CONCLUSIONS	13
LIST OF SYMBOLS	15
LIST OF REFERENCES	16
TABLES 1 and 2	18-20
ILLUSTRATIONS Figs. 1-9	
DETACHABLE ABSTRACT CARDS	

Table

LIST OF TABLES

1	Experimental pressure coefficients $M = 6.85$	18
2	Experimental pressure coefficients $M = 8.60$	20

LIST OF ILLUSTRATIONS

	<u>Fig.</u>
Experimental and theoretical values of pressure coefficient on cones at zero incidence at $M = 6.85$	1
Comparison of experimental pressure distributions with values calculated from the M.I.T. tables	2
Comparison of experimental pressure distributions with values calculated from the Laval shock-layer theory, modified to give the same $(C_p)_{\alpha=0}$ as the M.I.T. tables	3
Comparison of experimental pressure distributions with values calculated from Newtonian theory	4
Impact coefficients for 25° and 30° cones at $M = 6.85$	5
Impact coefficients for 35° and 45° cones at $M = 6.85$	6
Impact coefficients for 28° and 30° cones at $M = 8.60$	7
Impact coefficients for 30° and 40° cones at $M = 3.53$	8
Impact coefficients: summary of available data $3.53 < M < 8.60$	9

1 INTRODUCTION

A programme of tests is currently under way in the 7 in. x 7 in. hypersonic wind tunnel on the lifting properties of geometrically slender body shapes over a wide range of angles of incidence^{1,2}. Many of the shapes in this programme are either conical bodies of non-circular cross section, or bodies of revolution, and when analysing pressure distribution measurements for these bodies, the distribution on the related circular cone may be wanted as a basis of comparison. However, experimental information on pressure distributions on circular cones at hypersonic Mach numbers is extremely limited, most available results being for high supersonic speeds^{3,4,5}. Pressure distribution measurements were therefore made on five pointed cones with total apex-angles ranging from 25 to 45 degrees, at a Mach number of 6.85 (with a few tests at $M = 8.60$), over an incidence range of 0 to 30 degrees, and these distributions compared with values calculated from existing analytical and empirical theories. It is known, though, that all these theories for cones at incidence suffer, in one way or another, from the disability of not being based on an adequate model of the flow. To obtain such a model, more than pressure measurements are needed; for example, reliable measurements of flow direction and velocity on the surface and in the shock-layer would make it possible to determine the various regions in the mixed flow. Until such measurements, as well as an adequate theory which is more soundly based on a realistic model of the flow, are available, a full analysis cannot be made. For the time being therefore, one is restricted for cones at incidence to comparing results with approximate or empirical methods of calculation.

2 DESCRIPTION OF TESTS

The tests were made in the R.A.E. 7 in. x 7 in. hypersonic wind tunnel at a Mach number of 6.85, with a few repeat tests at $M = 8.60$. All tests were at a nominal stagnation pressure of 750 p.s.i.g., and a stagnation temperature sufficient to avoid liquefaction of the air in the test section. Under these conditions, a Reynolds number of 0.5 million per inch was obtained at $M = 6.85$, and 0.2 million per inch at $M = 8.60$. The cone models varied in length from 5 in. for the 25 degree cone, to 4.5 in. for the 45 degree cone.

Due to limited space in the model support mechanism, only seven $1\frac{1}{2}$ mm O.D. hypodermic pressure tubes could be led out from the model (smaller bore tubing was not used because of its greater pressure lag). Pressure tappings on each model surface were at a cross-section two-thirds of the model length from the apex, and were disposed 0, 15, 30, 60, 90, 135 and 180 degrees from the most-windward generator.

Pressures were measured on a conventional multi-tube mercury manometer bank, with one tube referred either to a Midwood absolute manometer, or a vacuum reference. Steady readings were obtained after some 10 to 15 seconds running, when the manometer was clamped and the tunnel shut down. Pressure measurements were obtained at angles of incidence of 0, 3, 6, 12, 18, 24 and 30 degrees; the results are presented in pressure coefficient form in Tables 1 and 2.

Evidence suggests that manometer readings were measured to an accuracy of ± 0.02 in Hg, which, with a similar error in reading the reference pressure corresponds to ± 0.003 in pressure coefficient, C_p , at $M = 6.85$, and ± 0.008

in C_p at $M = 8.60$. Errors in setting model incidence could amount to a further error in C_p of about ± 0.002 . The possible total direct measuring error is therefore ± 0.005 in C_p at $M = 6.85$ and ± 0.010 at $M = 8.60$. Additional to this measuring error, is the error arising from the lack of flow uniformity in the test section, the variation of $\frac{1}{2}\rho V^2$ in the region of the model being within $\pm 1\%$.

3 METHODS OF CALCULATING INVISCID SURFACE PRESSURE DISTRIBUTIONS

3.1 General

At the present time no exact method for calculating pressure distributions exists, except for the case of cones at zero incidence⁶. The aim of this section is to briefly recall the main features of the methods which have been put forward over the last 15 years, and to discuss the practical limitations in their use; a detailed discussion of the flow cannot be undertaken at this stage, because the measurements are not complete enough. For convenience, a common notation is used throughout this section, rather than the notation in the original papers.

3.2 The M.I.T. tables

The three sets of tables prepared in 1947-1949 at the Massachusetts Institute of Technology under the direction of Kopal, give solutions for zero incidence (based on the Taylor-Maccoll theory⁶), first-order corrections for incidence, and second-order corrections for incidence, respectively^{7,8,9}, the main assumptions being that the flow is inviscid and that there are no flow separations.

The formula for the pressure distribution is

$$\frac{p}{\bar{p}} = 1 + \alpha \frac{\eta}{\bar{p}} \cos \phi + \alpha^2 \left[\frac{\eta'}{\bar{p}} + \frac{\eta''}{\bar{p}} \cos 2\phi \right] \quad (1)$$

where $\frac{\eta}{\bar{p}}$ 1st order perturbation coefficient

and $\frac{\eta'}{\bar{p}}$, $\frac{\eta''}{\bar{p}}$ 2nd order perturbation coefficients

are dependent on Mach number and cone semi-angle (α)

α angle of incidence

ϕ meridional angle, measured from the windward generator

p absolute pressure

\bar{p} absolute pressure on cone at zero incidence.

It should be noted that the results are not tabulated in the most convenient system for practical use, being in wind-coordinates rather than body-coordinates. This can be remedied by a transformation of coordinates, as described by Roberts and Riley¹⁰. Another difficulty is that the number of tabulated solution of the second-order perturbation coefficients for the higher Mach numbers and cone angles is meagre, with the result that interpolation of values at Mach numbers different to those tabulated is rather inexact.

First-order theory is inadequate for predicting pressure distributions, its most obvious deficiencies being:-

(i) It gives an antisymmetrical variation of pressure about $\phi = 90^\circ$, additional to the zero-incidence pressure. This is not borne out by experiment,³ where it was found that the pressure at the $\phi = 90^\circ$ position varied with incidence; also the rate of increase of pressure with incidence at the $\phi = 0^\circ$ position was greater than the rate of decrease at $\phi = 180^\circ$.

(ii) It predicts no change in overall axial force with incidence, which again, is not borne out by experiment³.

Inclusion of the second-order term largely removes the above criticisms, but even so, a noticeable discrepancy between theory and experiment develops as the angle of incidence approaches the cone semi-angle³. It will be seen later that this is partly due to the third-order term no longer being negligible.

3.3 Shock-layer theories

These theories^{11,12,13}, are based on the Newtonian assumption of a thin shock layer surrounding the body surface, which pertains to the limiting situation of $M \rightarrow \infty$, and $\frac{\gamma-1}{\gamma+1} \rightarrow 0$, but theories are subsequently applied to other values of M and γ . Also, it is implicit in the development of these theories that the cone incidence is less than the cone semi-angle. The theory of Laval¹¹ is to third order in incidence; the theories of Guiraud¹² and Cheng¹³ are to second-order in incidence, but with a first-order correction for finite Mach number and density ratio. Expressions derived in these theories for pressure coefficient, C_p , are given below.

(1) Laval¹¹

$$\frac{1}{2} C_p = \sin^2 \epsilon + \alpha (\sin 2\epsilon \cos \phi) + \alpha^2 \left[\cos 2\epsilon - \sin^2 \phi \left(\cos^2 \epsilon + \frac{1}{4} \right) \right] - \alpha^3 \left[\frac{2}{3} \sin 2\epsilon \cos \phi + \frac{\sin 2\phi}{5 \sin 2\epsilon} \left(\sin \phi - \frac{\sin \epsilon}{2} \right) \right] \quad (2)$$

(ii) Guiraud¹²

$$\begin{aligned}
 \frac{1}{2} C_p &= \sin^2 \epsilon \left[1 + \frac{\bar{\gamma}-1}{4(\bar{\gamma}+1)} \right] + \frac{1}{M^2} \left(1 + \frac{1}{4} \frac{\bar{\gamma}-1}{\bar{\gamma}+1} \frac{\gamma+1}{\gamma-1} \right) \\
 &+ \alpha \cos \phi \left[2 \sin \epsilon \cos \epsilon - \frac{\gamma-1}{\gamma+1} \left(-\frac{4}{15} + \frac{1}{2} \sin^2 \epsilon \right) \tan \epsilon - \frac{7}{30} \frac{\bar{\gamma}-1}{\bar{\gamma}+1} \frac{\gamma+1}{\gamma-1} \frac{1}{M^2 \sin \epsilon \cos \epsilon} \right] \\
 &+ \alpha^2 \left[\cos 2\epsilon + \frac{\bar{\gamma}-1}{\bar{\gamma}+1} \left(\frac{-7}{60 \cos^2 \epsilon} - \frac{29}{60} + \frac{1}{2} \cos^2 \epsilon \right) + \frac{\bar{\gamma}-1}{\bar{\gamma}+1} \frac{\gamma+1}{\gamma-1} \frac{1}{M^2 \sin^2 \epsilon \cos^2 \epsilon} \left(\frac{7}{60} - \frac{7}{30} \sin^2 \epsilon \right) \right] \\
 &+ \left[-\cos^2 \epsilon - \frac{1}{4} + \frac{\bar{\gamma}-1}{\bar{\gamma}+1} \left(\frac{-53}{120 \cos^2 \epsilon} + \frac{17}{60} - \frac{1}{4} \cos^2 \epsilon \right) + \right. \\
 &\left. + \frac{\bar{\gamma}-1}{\bar{\gamma}+1} \frac{\gamma+1}{\gamma-1} \frac{1}{M^2 \sin^2 \epsilon \cos^2 \epsilon} \left(\frac{17}{32} - \frac{467}{480} \sin^2 \epsilon \right) \right] \sin^2 \phi \quad (3)
 \end{aligned}$$

In the above expression, γ has the usual value of 1.4, but $\bar{\gamma}$ is a fictitious mean adiabatic index chosen so as best to represent the thermodynamic properties of the gas downstream of the shock wave.

(iii) Cheng¹³

$$\begin{aligned}
 \frac{C_p}{2 \sin^2 \epsilon} &= 1 + \frac{\gamma-1}{\gamma+1} \left(\frac{1+5\kappa}{4} \right) + \left(\frac{\gamma-1}{\gamma+1} \right)^2 \left[\frac{3}{32} (1+\kappa)^2 - \frac{\kappa^2}{2} + \frac{\tan^2 \epsilon}{4} (1+\kappa)^2 - \frac{(1+\kappa)}{2} \log (1+\kappa) \right] \\
 &+ 2 \frac{\sin \alpha}{\sin \epsilon} \cos \epsilon \cos \phi + \left(\frac{\sin \alpha}{\sin \epsilon} \right)^2 \left[\cos 2\epsilon - \sin^2 \phi \left(\cos^2 \epsilon + \frac{1}{4} \right) \right] \\
 &- \frac{\gamma-1}{\gamma+1} \frac{\sin \alpha}{\sin \epsilon} \left[-\frac{4}{15} (1+\kappa) + \frac{\sin^2 \epsilon}{2} - \frac{\kappa}{2} \cos 2\epsilon \right] \frac{\cos \phi}{\cos \epsilon} \quad (4)
 \end{aligned}$$

In the above expression, $\kappa = \frac{\gamma+1}{\gamma(\gamma-1)M^2 \sin^2 \epsilon}$.

For $\alpha = 0$, with $\gamma \rightarrow 1$ and $M \rightarrow \infty$, the three theories all reduce to the simple Newtonian expression $C_p = 2 \sin^2 \epsilon$; with $\gamma = 1.4$ and $M \rightarrow \infty$, the theories of Guiraud and Cheng reduce to $C_p = 2.083 \sin^2 \epsilon$.

For small finite values of α (i.e. $\sin \alpha \simeq \alpha$), with $\gamma \rightarrow 1$ and $M \rightarrow \infty$, the theories of Guiraud and Cheng reduce to the Laval theory to the second-order in incidence. As an indication of the range of incidence over which these theories are applicable, it should be noted that the α^2 -term in the Laval theory becomes significant when the incidence is as great as the cone semi-angle, the α^3 -term accounting for some 2% of the pressure coefficient at $\phi = 0$ when $\alpha = \epsilon$.

3.4 Empirical methods

Since it was shown in Section 3.3 that analytical theories can only be expected to be relevant to a limited range of incidence, one is at present forced to rely on empirical methods if large angles of incidence are considered. The most well-known method is based on the simple Newtonian "impact" concept, which gives the pressure coefficient at a point on a surface whose local incidence to the free stream is θ , as $C_p = 2 \sin^2 \theta$. For a cone, the value of θ is given by

$$\sin \theta = \sin \epsilon \cos \alpha + \cos \epsilon \sin \alpha \cos \phi \quad (5)$$

For angles of incidence greater than the semi-angle of the cone, part of the cone surface cannot be regarded as being subject to an impact flow. The boundary between the two regions is found by equating $\sin \theta$ to zero in the above expression, which gives

$$(\cos \phi)_{ER} = - \frac{\tan \epsilon}{\tan \alpha} \quad (6)$$

In this "shadow" region, where $\phi > \phi_{ER}$, the impact concept has no meaning, and the usual assumption for hypersonic speeds is that the pressure on this region of the cone surface is the same as that of the free stream, i.e. $C_p = 0$. The minimum value possible for pressure in this region is, of course, that of vacuum, and this corresponds to a pressure coefficient, $C_{PVAC} = - \frac{2}{\gamma M^2}$.

However, the use of the Newtonian method for real air is open to criticism, the original Newtonian concept being based on perfectly elastic fluid particles, and certain refinements of the Newtonian concept have been proposed for real air according to the type of body under consideration, but still limited to the case of very high Mach number. These expressions are derived in Ref. 14, but are summarised below for convenience:-

For an attached conical shock,

$$C_p = \frac{2(\gamma+1)(\gamma+7)}{(\gamma+3)^2} \sin^2 \theta = 2.083 \sin^2 \theta \quad (7)$$

For a blunt body with detached shock,

$$C_p = \frac{(\gamma+3)}{(\gamma+1)} \sin^2 \theta = 1.83 \sin^2 \theta \quad (8)$$

for
 $\gamma = 1.4$

The latter expression is generally referred to as "modified-Newtonian" theory. Both expressions reduce to $C_p = 2 \sin^2 \theta$ when $\gamma = 1$.

Mention must also be made of the equivalent-cone (or tangent-cone) method, which also depends on the concept of local surface incidence. In this method, the assumption is made that the pressure at a point on the cone surface where the local incidence is θ , is the same as that on a cone of semi-angle θ , at zero incidence. This method is limited to values of θ less than 57.5° , this angle being the maximum possible cone semi-angle for shock attachment at $M = \infty$.¹⁴ For $M = \infty$, it gives $C_p = 2.083 \sin^2 \theta$; for all finite Mach numbers, it gives $C_p > 2.083 \sin^2 \theta$.

The variety of modifications to the Newtonian concept just described suggests a more generalised form of impact theory, $C_p = K \sin^2 \theta$, where K is an "impact coefficient" dependent on local surface incidence and Mach number. For instance, in the case of infinite Mach number, one would expect K to vary between 2.083 and 1.83 as the local incidence on the cone surface varied from 0 to 90 degrees; at finite Mach numbers, K would probably vary between wider limits. The experimental results reported in this Note have been analysed on this basis, the measured pressure coefficients (given in Tables 1 and 2) being reduced to impact coefficients by dividing them by $\sin^2 \theta$. (Figs. 5-9).

4. COMPARISON OF RESULTS WITH AVAILABLE METHODS FOR CALCULATING PRESSURE DISTRIBUTIONS

4.1 Cones at zero incidence

The variation of pressure coefficient with cone semi-angle, at a Mach number of 6.85 and zero incidence, is shown in Fig. 1. The plotted symbols indicate the spread of results from the seven pressure tappings on each model. Excellent agreement is obtained between the measured pressure coefficients and values calculated from the theory of Taylor and Maccoll^{6,7}. Newtonian theory and Laval theory¹¹ ($C_p = 2 \sin^2 \epsilon$), and the theories of Guiraud¹² and Cheng¹³ for $M = \infty$ and $\gamma = 1.4$ ($C_p = 2.083 \sin^2 \epsilon$), all give underestimates of pressure coefficient. On the other hand, the latter theories^{12,13} with a first-order correction for finite Mach number give over-estimates of pressure coefficient. A peculiarity of the theory of Guiraud is that for a finite Mach number, a finite pressure coefficient is obtained for zero cone angle.

It is clear, therefore, that the shock-layer theories^{11,12,13} in their present form cannot give accurate estimates of the pressure distribution on

a cone at incidence, except by accident, since they depend on the addition of terms in α , α^2 and α^3 to the value of the pressure coefficient on the cone at zero incidence - which is incorrectly estimated by these theories. However, this inconsistency can be removed by adding the α -terms of the shock-layer theories instead to values of $(C_p)_{\alpha=0}$ calculated from the theory of Taylor and Maccoll^{6,7}; this is discussed further in para. 4.2.2.

4.2 Cones at incidence

Experimental values of pressure coefficient for five cones with apex angles ranging from 25 to 45 degrees, at angles of incidence up to 30 degrees, are given in Tables 1 and 2. To simplify matters, only the results for the 30 degree cone are discussed in detail in this section, it being understood that, unless stated otherwise, all conclusions apply qualitatively to the whole range of cone angles tested.

4.2.1 Comparison with the M.I.T. tables^{7,8,9}

Pressure distributions on the 30 degree cone, at a Mach number of 6.85, are compared in Fig. 2 with values calculated from the M.I.T. tables for angles of incidence of 0, 6, 12, 18 and 24 degrees. It can be seen that the shape of the pressure distribution around the cone cross-section is not accurately predicted by this theory, pressures being consistently over-estimated for $0 < \phi < 45^\circ$, and under-estimated for $45^\circ < \phi < 180^\circ$. A similar difference between theory and experiment was reported in Ref. 3, for tests at a Mach number of 3.53, but in this case agreement was closer in the region $135^\circ < \phi < 180^\circ$ than in the present tests. The discrepancy between theoretical and experimental values is small for angles of incidence less than the semi-angle of the cone, but at higher angles of incidence this discrepancy increases rapidly, and the absurd prediction of negative absolute pressures on the leeward surface of the cone is obtained.

The experimental results show that at the higher angles of incidence, pressures on the leeward surface of the cone tend to free stream pressure (i.e. $C_p = 0$), rather than vacuum ($C_p = \frac{-2}{\gamma M^2}$). This is possibly due to viscous effects, but an approximate calculation, outlined below, shows that the difference is not accounted for by the simple assumption that the external flow is influenced only by the displacement effect of the boundary layer (the "weak-interaction" effect^{16,17}).

The significant parameter in calculating boundary-layer self-induced pressures is $\chi = \frac{M^3}{\sqrt{R_x}}$, where R_x is the local Reynolds number at the point under consideration. The induced pressure on a flat plate at zero incidence is given by¹⁷:-

$$\frac{P}{P_\infty} = 1 + \frac{\gamma}{2} \frac{\gamma-1}{\gamma+1} \left(0.664 + 1.73 \frac{T}{T_s} \right) \chi \quad (9)$$

This formula should apply approximately to the case of a cone at an incidence equal to its semi-angle (i.e. $\alpha = \epsilon$) in the region of $\phi = 180^\circ$, i.e. when the most-leeward generator is aligned with the free stream. If

we take $\frac{T_w}{T_s} = 0.5$, which is a mean between the two extreme cases of an insulated surface and a very cold wall, we get:-

$$M = 6.85 : \frac{p}{p_\infty} = 1.05, \quad \text{or} \quad \Delta C_p = 0.0015$$

$$M = 8.60 : \frac{p}{p_\infty} = 1.14, \quad \text{or} \quad \Delta C_p = 0.0025.$$

A comparison of pressure coefficients in the $\phi = 180$ degree region for the 30 deg. cone at Mach numbers of 6.85 and 8.60 in Tables 1 and 2, shows that the difference in C_p at the two Mach numbers is about 0.030, i.e. some ten times greater than that predicted by the weak-interaction formula. Therefore, if viscous effects are to account for the discrepancies, they may be of a different nature from those assumed. It is clear that further experiments are needed to gain an understanding of the combined effects of Reynolds number and Mach number, on the pressure on those regions of a cone where the local incidence is small.

4.2.2 Comparison with the shock-layer theories^{11,12,13}

A comparison of pressure distributions calculated from the theories of Laval, Guiraud and Cheng (Equations 2,3 and 4 respectively) shows that they all give $C_p - \phi$ distributions of nearly the same shape, but with noticeable differences in absolute values of C_p . This is due mainly to the quite large differences in values of $(C_p)_{\alpha=0}$ obtained from these theories (Fig. 1), rather than differences in the α and α^2 -terms. This is illustrated below, where values appropriate to a 30 degree cone and a Mach number of 6.85 have been substituted in equations 2,3 and 4.

Laval

$$C_p = 0.134 + \alpha \cos \phi + \alpha^2 (1.73 - 2.37 \sin^2 \phi)$$

to the second-order in α , and for $M = \infty$.

Guiraud

$$C_p = 0.193 + 0.98 \alpha \cos \phi + \alpha^2 (1.75 - 2.19 \sin^2 \phi).$$

Cheng

$$C_p = 0.170 + 0.92 \sin \alpha \cos \phi + \sin^2 \alpha (1.73 - 2.37 \sin^2 \phi).$$

The corresponding expression calculated from the M.I.T. tables (equation 1) is

$$C_p = 0.148 + 0.98 \alpha \cos \phi + \alpha^2 (1.7 - 2.4 \sin^2 \phi)$$

and the coefficients in the second-order term are quoted to only two significant figures, because of the difficulties of interpolation from the M.I.T. tables at a Mach number as high as 6.85.

Inspection of the above formulae reveals that there is no great difference between the coefficients of either the α -terms, or the α^2 -terms, and if a common value of $(C_p)_{\alpha=0}$ were used, approximately the same values would be obtained from all four expressions for the $C_p - \phi$ distribution. For this reason, no separate plots giving comparisons of experimental pressure distributions, and distributions calculated from the shock-layer theories, are given in this Note. Since it has been found that the M.I.T. tables^{6,7} give the best estimates of $(C_p)_{\alpha=0}$, and α and α^2 -terms little different to the shock-layer theories, there would seem to be no advantage in using the second-order shock-layer theories. However, as mentioned in section 3.2, accurate interpolation of the second-order perturbation coefficients at high Mach numbers from the M.I.T. tables is difficult, and if there was the need for programming large numbers of calculations on a computer the shock-layer theories might be more convenient for calculating the α^2 -terms.

Before leaving shock-layer theories, further mention should be made of the Laval theory. This theory suffers from being restricted to $M = \infty$, but unlike the other theories, is to third-order in incidence. A comparison of experimental pressure distributions with values calculated from the Laval theory (but using the correct value of $(C_p)_{\alpha=0}$) is given in Fig. 3. It can be seen that the discrepancy between theoretical and experimental values is reduced by inclusion of the third-order term, as compared with second-order theories, but for angles of incidence less than the semi-angle of the cone the effect is small. Part of the advantage of including the third-order term is lost through the Laval theory being restricted to $M = \infty$, and there is a case for adding this third-order term instead to the pressure distributions calculated to the second-order in α from the M.I.T. tables.

4.2.3 Comparison with empirical theories

Experimental pressure distributions are compared with values calculated from impact theory ($C_p = 2 \sin^2 \theta$) in Fig. 4. At low angles of incidence this theory under-estimates pressures, but over-estimates them at the higher angles of incidence ($\alpha > \epsilon$). Modified-Newtonian theory ($C_p = 1.83 \sin^2 \theta$) would give a better estimate for the higher angles of incidence, but at the expense of an increased under-estimate at low angles. Nevertheless, both of these theories give closer estimates of pressure distributions at high angles of incidence than is obtained from the M.I.T. tables.

It has already been suggested in section 3.4 that a more general form of impact theory, $C_p = K \sin^2 \theta$, might be more appropriate, where K is an "impact coefficient" which is a function of the local incidence, θ , and Mach number. The comparison of theoretical and experimental pressure distributions in Fig. 4

tends to support this possibility, since the theoretical estimates change from an under-estimate to an over-estimate as the cone incidence increases. The values of C_p in Tables 1 and 2 have therefore been reduced to impact-coefficient form by dividing them by $\sin^2 \theta$, and the values of impact coefficient obtained are plotted in Figs. 5, 6 and 7. The shaded area at the bottom of each figure shows the range over which scatter can be attributed to experimental error (see section 2). Results from tests at a lower Mach number³ have been analysed in the same way and are plotted in Fig. 8, in this case the degree of experimental scatter is not known. The results of Figs. 5-8 are summarised in Fig. 9, which also includes some results from Refs. 4 and 5 for large values of local incidence.

With few exceptions, the experimental results fall within a band whose width is no greater than the expected range of experimental scatter, showing that the impact concept of using the local incidence, θ , relates quite well the combined effects of cone incidence, α , cone semi-angle, ϵ , and meridional position on the cone surface, ϕ , and that the impact coefficient, K , is dependent on θ . It is found that for the Mach numbers of the present tests that K varies from about 2.5 at $\theta = 10$ degrees, to about 1.9 at $\theta = 50$ degrees, the highest value of local incidence reached. The results from tests at a Mach number of 3.53 (Fig. 8), show slightly higher values of K for values of θ less than about 40 degrees. For values of θ less than 10 degrees, K is apparently increasing rapidly, but so too is the experimental error, and values of K in this range of θ cannot be accurately estimated.

In the summary of results in Fig. 9, results for $\phi = 0$ degree only have been plotted in order to avoid a confusion of plotted points; this is justified since the results in Figs. 5-8 show no isolated effect of ϕ on K . In Fig. 9 a comparison is made between the experimental results and values calculated by three empirical methods:- equivalent cone, Newtonian and modified-Newtonian (previously described in section 3.4). It is clear that the Newtonian and modified-Newtonian expressions, which give a constant value of impact coefficient, are unrealistic, and can only apply over a limited range of local incidence with acceptable accuracy. Thus Newtonian theory is accurate to within a few per cent over the range $25^\circ < \theta < 45^\circ$, and modified-Newtonian theory within a few per cent for $70^\circ < \theta < 90^\circ$. The equivalent-cone method has the merit of predicting a variation of K with local incidence and Mach number, but with reasonable accuracy only for $\theta < 25$ degrees.

Thus no single empirical method is satisfactory for the whole range of local incidence from 0 to 90 degrees. However, a mean curve could be drawn through the experimental points in Fig. 9, and if an empirical method must be used (as would seem to be the case for $\alpha > \epsilon$), values of K taken from this curve would be preferable to using values of K calculated from any one of the previously mentioned empirical methods. It must be emphasised though, that the $K - \theta$ variation in Fig. 9 applies only to circular cones, and not to any other body shapes such as conical bodies of non-circular cross-section.

5 CONCLUSIONS

From experiments at Mach numbers of 6.85 and 8.60 on cones with total apex-angles ranging from 25 to 45 degrees, the following conclusions can be

made regarding the extent to which various analytical and empirical theories predict the pressure distribution on a circular cone.

(1) Cones at zero angle of incidence

Excellent agreement was obtained between the measured pressures and values calculated from the M.I.T. tables⁷ based on the theory of Taylor and Maccoll⁶. Of the shock-layer theories, the Laval theory gives under-estimates of pressure, while the theories of Guiraud and Cheng give over-estimates. These discrepancies mean that the shock-layer theories, in their present form, cannot give adequate estimates of the pressure distribution on a cone at incidence, since this estimate is dependent on the addition of terms in incidence, and $(\text{incidence})^2$, to the zero-incidence value. This inconsistency can be removed by adding the incidence-terms of these theories instead to values for zero incidence calculated from the M.I.T. tables⁷.

(2) Cones at incidence

(i) The shape of the pressure distribution is not accurately predicted by values calculated from the M.I.T. tables. The difference between theoretical and experimental estimates is small for angles of incidence less than the cone semi-apex angle, but rapidly increases at higher angles of incidence. This is to be expected, since terms higher than the second-order are no longer negligible under these conditions.

(ii) If values of pressure at zero incidence calculated from the M.I.T. tables are used, estimates of pressure distributions calculated from the shock-layer theories are not significantly different from each other, or from distributions calculated from the M.I.T. tables, for angles of incidence less than the cone semi-apex angle. Since for hypersonic Mach numbers interpolation of the coefficients of the incidence-terms from the M.I.T. tables is difficult, it may be easier, and apparently no less accurate, to calculate these coefficients instead from one of the shock-layer theories.

For Mach numbers lower than those of the present tests, the Laval theory would become inadequate, this theory being unable to account for finite Mach number. Although not checked in the present tests, it is likely that the first-order corrections for Mach number in the theories of Guiraud and Cheng would become inadequate at low supersonic Mach numbers.

(iii) For angles of incidence higher than the semi-apex angle of the cone, analytical theories cannot be expected to apply, it being implicit in their development that $\alpha < \epsilon$, and one is forced to rely on empirical methods if large angles of incidence are considered. An empirical analysis of the experimental pressure distributions reveals that the pressure at a point on a cone surface is dependent on the local incidence of the surface at that point to the free stream, this local incidence, θ , relating quite well the combined effect of cone incidence, cone semi-apex angle, and meridional position on the cone surface. It follows that if the measured pressure coefficients are divided by the appropriate values of $\sin^2 \theta$ to give an "impact coefficient", K , an approximately defined single curve of K versus θ is obtained for each Mach number, though the effect of Mach number is small. This variation of K with θ embraces values of K calculated by the equivalent-cone, Newtonian, and modified-Newtonian methods

but each only over limited ranges of θ , which shows that the use of any one of these methods on its own over a large range of θ is unrealistic.

(3) Further experiments are needed to obtain pressures to greater accuracy in the "shadow" regions on the cone surface, which occur when the cone incidence is greater than the cone semi-apex angle, and also to greater accuracy on those parts of the cone surface where the local incidence is small. This could be achieved by the use of oil manometers, rather than the mercury manometers used in the present tests, and this will be investigated in the future.

(4) Altogether, it has been demonstrated for the range of cone angles tested that existing analytical theories only predict pressures on the surfaces of lifting cones with reasonable accuracy for a limited range of angles of incidence and Mach number. For higher angles of incidence, even though an impact coefficient can be used to correlate the pressure coefficients, once they have been measured, there is no reason to assume that the same relation between impact coefficient and surface slope applies to any shape other than circular cones. Future work must, therefore, be directed towards a more complete exploration of the flow field, from which one may hope to derive a more realistic model of the flow, as a basis for better methods of prediction.

LIST OF SYMBOLS

M	free stream Mach number
K	impact coefficient = $\frac{C_p}{\sin^2 \theta}$
T	absolute temperature
p	absolute pressure on cone surface
\bar{p}	absolute pressure on cone surface at zero incidence
$\frac{\eta}{\bar{p}}, \frac{\eta'}{\bar{p}}, \frac{\eta''}{\bar{p}}$	perturbation coefficients given in M.I.T. tables
α	angle of incidence of cone axis
ϵ	cone semi-apex angle
ϕ	meridional position on cone surface measured from the most windward generator
θ	local surface incidence
γ	ratio of specific heats
$\bar{\gamma}$	fictitious ratio of specific heats in Guiraud's theory chosen so as best to represent the thermodynamic properties of the gas downstream of the shock wave

$$\kappa = \frac{\gamma + 1}{\gamma(\gamma-1)M^2 \sin^2 \epsilon}$$

$$\chi = \frac{M^3}{\sqrt{R_x}} \text{ where } R_x \text{ is the local Reynolds number}$$

$$C_p \text{ pressure coefficient} = \frac{p - p_\infty}{\frac{\gamma}{2} p_\infty M_\infty^2}$$

Suffixes

- w wall value
s stagnation value
 ∞ free stream conditions
ER expansion region
VAC vacuum conditions

LIST OF REFERENCES

- | <u>No.</u> | <u>Author</u> | <u>Title etc.</u> |
|------------|----------------------------------|---|
| 1 | Peckham, D.H. | A proposed programme of wind tunnel tests at hypersonic speeds to investigate the lifting properties of geometrically slender shapes.
RAE Tech.Note Aero No.2730 ARC.22,594 December, 1960 |
| 2 | Crane, J.F.W.,
Crabtree, L.F. | The 7 in. x 7 in. hypersonic wind tunnel at RAE Farnborough. Parts I, II and III.
ARC. C.P. No. 590 . August, 1961. |
| 3 | Holt, M.,
Blackie, J. | Experiments on circular cones at yaw in supersonic flow.
Jnl.Aero.Sci.23 (10) October, 1956, 931. |
| 4 | Amick, J.L. | Pressure measurements on sharp and blunt 5° - and 15° - half-angle cones at Mach number 3.86 and angles of attack to 100°.
NASA TN D-753. February, 1961. |
| 5 | Conti, R.J. | Laminar heat-transfer and pressure measurements at a Mach number of 6 on sharp and blunt 15° half-angle cones at angles of attack up to 90°.
NASA TN D-962. October, 1961. |
| 6 | Taylor, G.I.,
Maccoll, J.W. | Air pressure on a cone moving at high speeds.
Proc. Royal Soc. A Vol.139, p.278-311 1933, |

LIST OF REFERENCES (Contd)

<u>No.</u>	<u>Author</u>	<u>Title etc.</u>
7	Kopal, Z.	Tables of supersonic flow around cones. Tech. Report No. 1 M.I.T. P.18356 1947
8	Kopal, Z.	Tables of supersonic flow around yawing cones. Tech. Report No. 3 M.I.T. 1947
9	Kopal, Z.	Tables of supersonic flow around cones of large yaw. Tech Report No. 5 M.I.T. 1949
10	Roberts, R.C., Riley, J.D.	A guide to the use of the M.I.T. cone tables. Jnl.Aero.Sci. <u>21</u> (5) May 1954, 336
11	Laval, P.	Ecoulements Newtoniens sur des surfaces conique en incidence. La Recherche Aeronautique No. 73, Nov-Dec 1959
12	Guiraud, J.P.	Newtonian flow over a surface. Colston Symposium on Hypersonic Flow, Bristol 1959
13	Cheng, H.K.	Hypersonic shock-layer theory of a yawed cone and other three-dimensional bodies. Jnl. Fl. Mech. <u>12</u> (2) 1962, 169
14	Crabtree, L.F.	Survey of inviscid hypersonic flow theory for geometrically slender shapes. Unpublished M.o.A. Report.
15	Ames Research Staff	Equations, tables, and charts for compressible flow. NACA Report 1135 1953
16	Bertram, M.H., Blackstock, T.A.	Some simple solutions to the problem of predicting boundary layer self-induced pressures. NASA TN D-798 April 1961
17	Cheng, H.K., Hall, J.G., Golian, T.C., Hertzberg, A.	Boundary layer displacement and leading edge bluntness effects in high temperature hypersonic flow. Jnl.Aero.Sci. <u>28</u> (5) May 1961, 353

TABLE 1

Experimental pressure coefficients. $M = 6.85$

25 deg. cone ($\epsilon = 12\frac{1}{2}$ deg.)

ϕ deg. \ a deg.	0	3	6	12	18	24	30
0	0.108	0.152	0.205	0.345	0.503	0.682	0.875
15	0.106	0.150	0.202	0.335	0.480	0.647	0.826
30	0.105	0.145	0.189	0.301	0.418	0.552	0.694
60	0.115	0.128	0.149	0.199	0.246	0.300	0.352
90	0.112	0.110	0.106	0.097	0.094	0.096	0.096
135	0.112	0.085	0.064	0.026	0.017	0.014	0.002
180	0.111	0.077	0.053	0.025	0.023	0.019	0.006

30 deg. cone ($\epsilon = 15$ deg.)

ϕ deg. \ a deg.	0	3	6	12	18	24	30
0	0.150	0.206	0.269	0.422	0.582	0.756	0.943
15	0.149	0.200	0.258	0.406	0.559	0.721	0.885
30	0.148	0.196	0.245	0.372	-	-	-
60	0.150	0.179	0.201	0.258	0.312	0.372	0.424
90	0.152	0.151	0.148	0.138	0.132	0.132	0.134
135	0.154	0.122	0.096	0.049	0.011	0.004	0.009
180	0.153	0.108	0.078	0.037	0.010	0.003	0.007

TABLE 1 (Contd)

35 deg. cone ($\epsilon = 17\frac{1}{2}$ deg.)

ϕ deg. \ / \ / α deg.	0	3	6	12	18	24	30
0	0.200	0.258	0.322	0.475	0.640	0.835	1.041
15	0.190	0.252	0.324	0.476	0.636	0.817	1.010
30	0.199	0.249	0.310	-	-	0.766	0.921
60	0.198	0.225	0.257	0.332	0.378	0.434	0.486
90	0.204	0.198	0.195	0.182	0.173	0.173	0.167
135	0.200	0.162	0.126	0.061	0.023	0.004	0.006
180	0.186	0.135	0.091	0.035	0.011	0	-0.005

45 deg. cone ($\epsilon = 22\frac{1}{2}$ deg.)

ϕ deg. \ / \ / α deg.	0	3	6	12	18	24	30
0	0.312	0.390	0.471	0.649	0.835	1.015	1.210
15	0.311	0.388	0.466	0.632	0.815	0.985	1.161
30	0.311	0.378	0.449	0.595	0.756	0.895	1.030
60	0.313	0.351	0.387	0.447	0.516	0.575	0.615
90	0.317	0.316	0.313	0.292	0.276	0.261	0.253
135	0.324	0.296	0.258	0.153	0.075	0.036	0.021
180	-	0.304	0.253	0.125	0.046	0.022	0.016

TABLE 2

Experimental pressure coefficients. M = 8.60

28 deg. cone ($\epsilon = 14^\circ$)

α deg. ϕ deg.	0	3	6	12	18	24	30
0	0.135	0.189	0.246	0.388	0.569	0.765	0.968
15	0.135	0.180	0.237	0.370	0.537	0.718	0.902
30	0.135	0.169	0.220	0.330	0.475	0.618	0.758
60	0.135	0.148	0.175	0.230	0.302	0.350	0.410

30 deg. cone ($\epsilon = 15^\circ$)

α deg. ϕ deg.	0	3	6	12	18	24	30
0	0.130	0.204	0.270	0.431	0.628	0.810	1.030
15	0.132	0.198	0.254	0.401	0.574	0.762	0.934
30	0.133	0.188	0.237	0.360	0.491	0.638	0.790
60	0.133	0.168	0.193	0.250	0.311	0.375	0.450
90	0.145	0.146	0.150	0.140	0.136	0.129	0.140
135	0.141	0.112	0.107	0.058	0.042	0.039	0.039
180	0.147	0.103	0.090	0.049	0.039	0.038	0.035

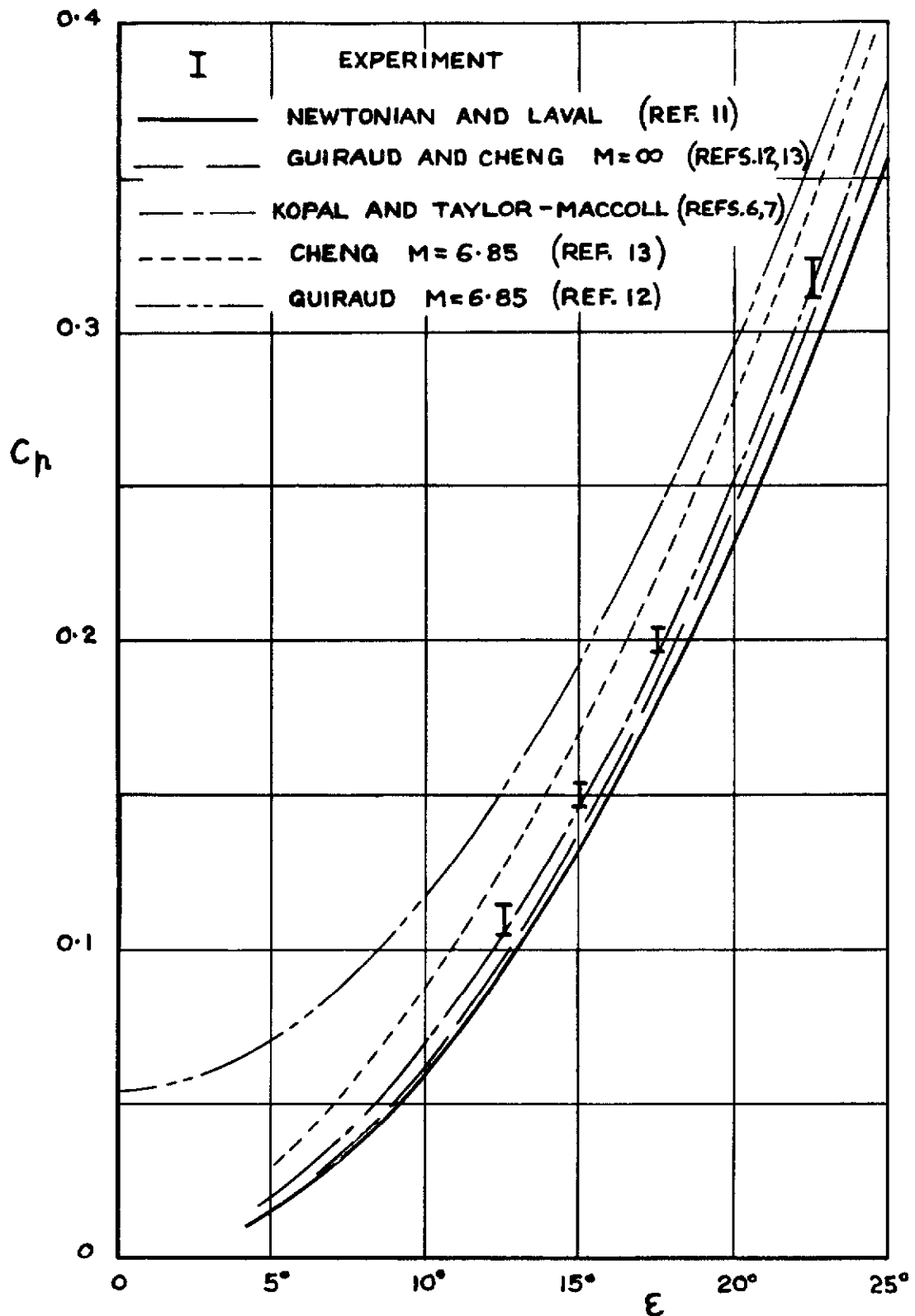


FIG.1 EXPERIMENTAL AND THEORETICAL VALUES OF PRESSURE COEFFICIENT ON CONES AT ZERO INCIDENCE AT $M=6.85$.

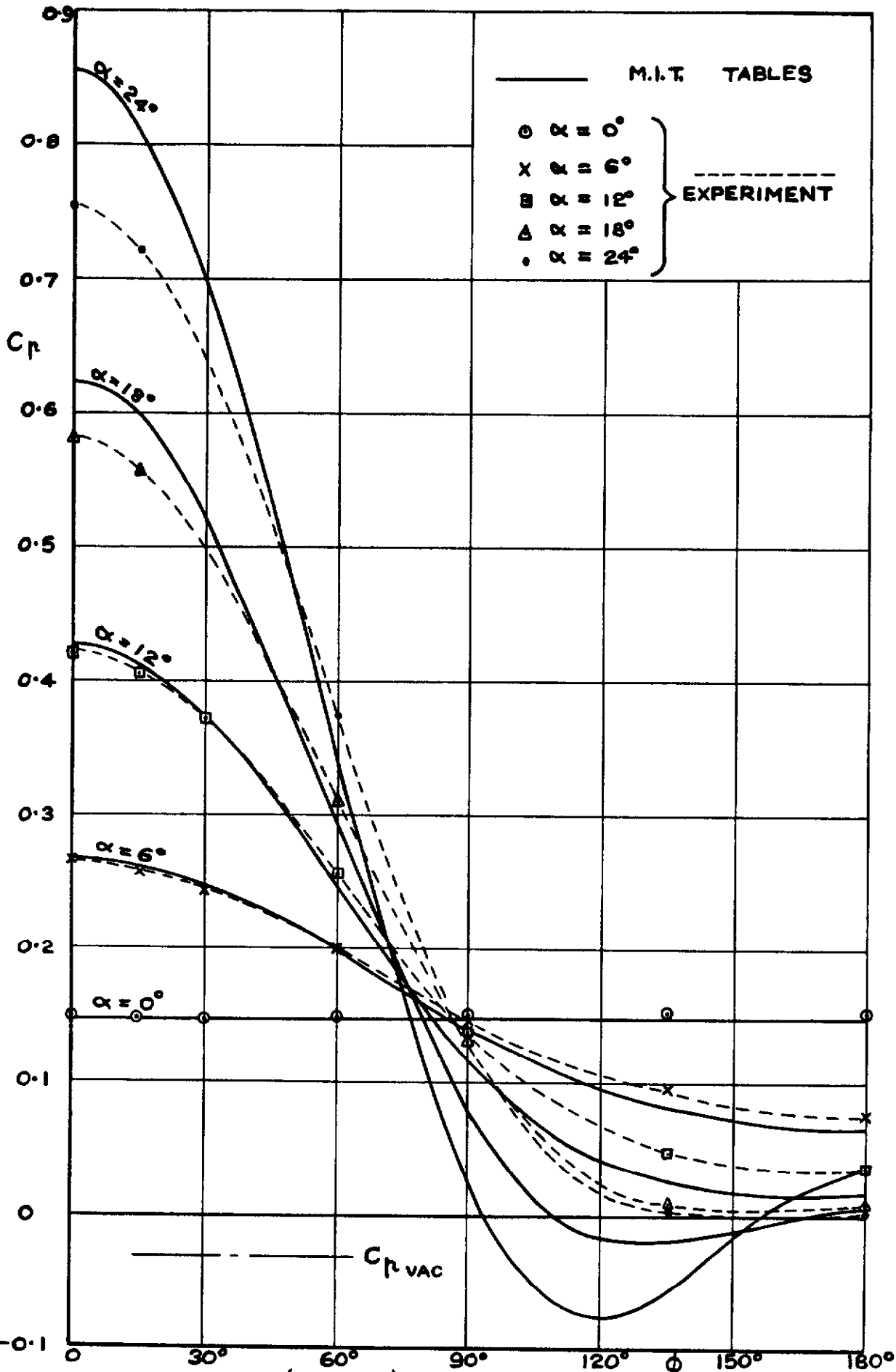


FIG. 2 30° CONE ($\epsilon = 15^\circ$) COMPARISON OF EXPERIMENTAL PRESSURE DISTRIBUTIONS WITH VALUES CALCULATED FROM THE M.I.T. TABLES (REFS. 7,8 & 9) $M = 6.85$.

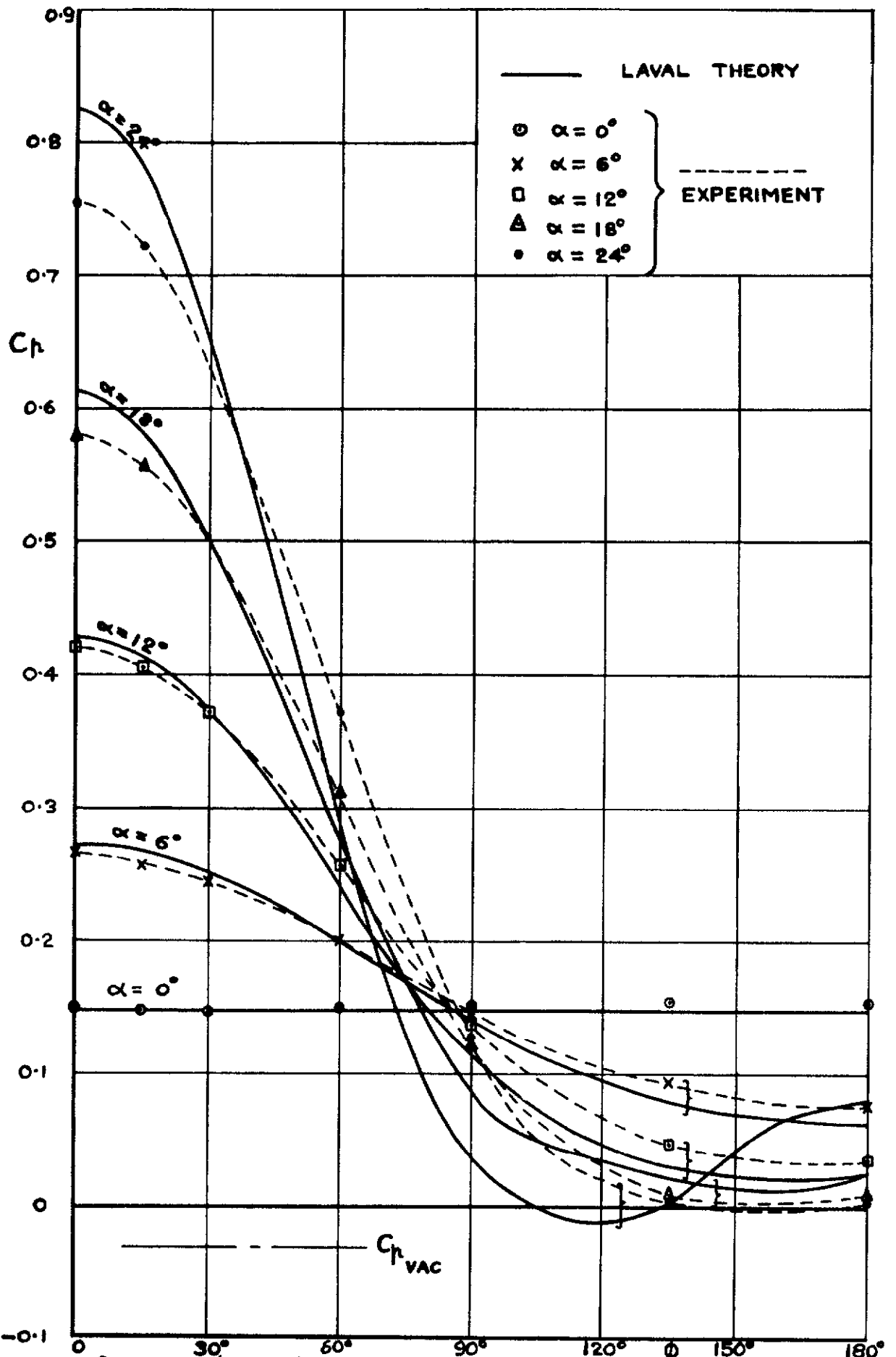


FIG.3 30° CONE ($\epsilon = 15^\circ$) COMPARISON OF EXPERIMENTAL PRESSURE DISTRIBUTIONS WITH VALUES CALCULATED FROM THE LAVAL SHOCK-LAYER THEORY (REF. II), MODIFIED TO GIVE THE SAME $(C_p)_{\alpha=0}$ AS THE M.I.T. TABLES.

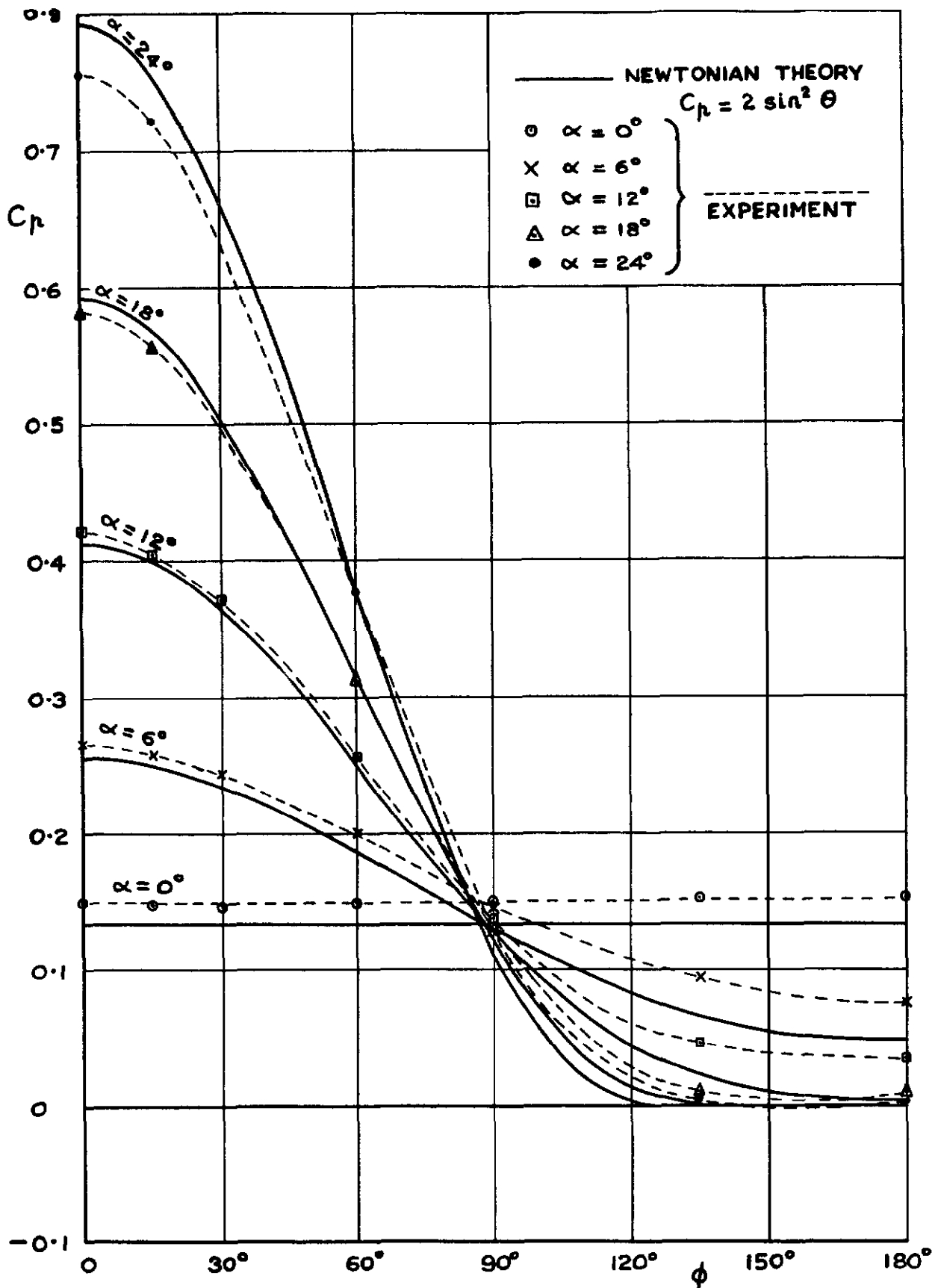
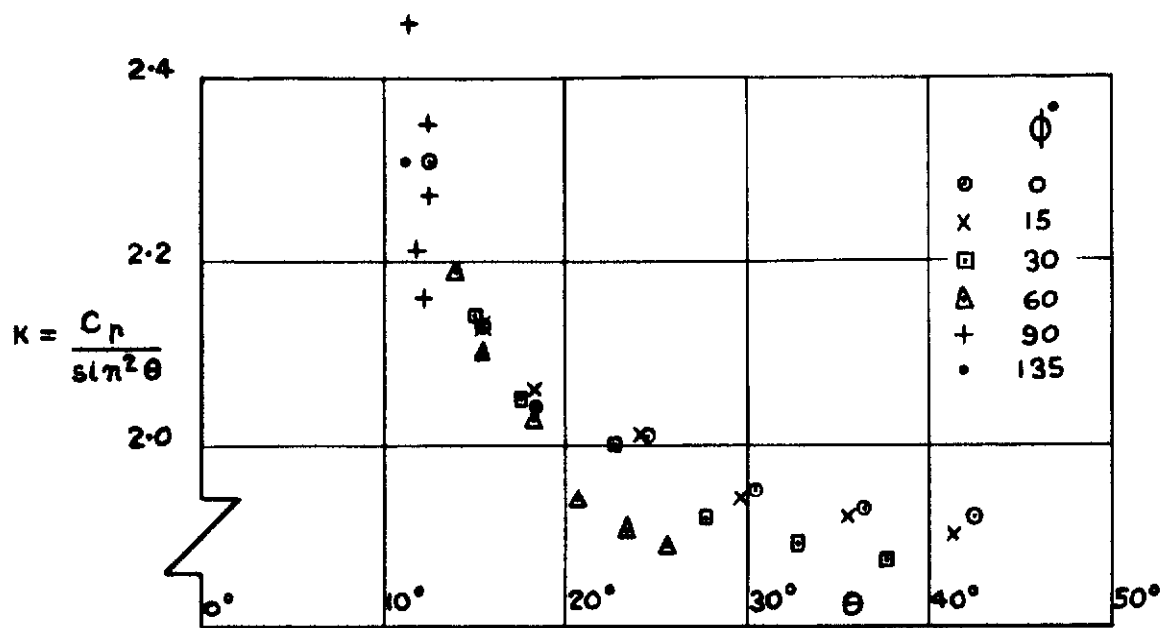
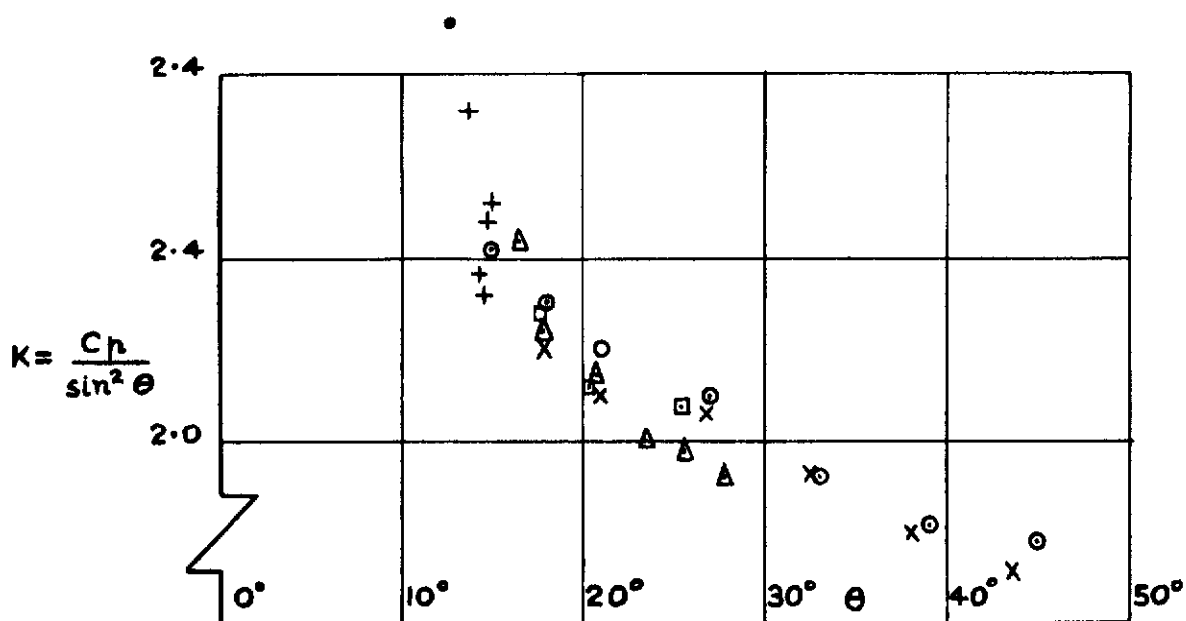


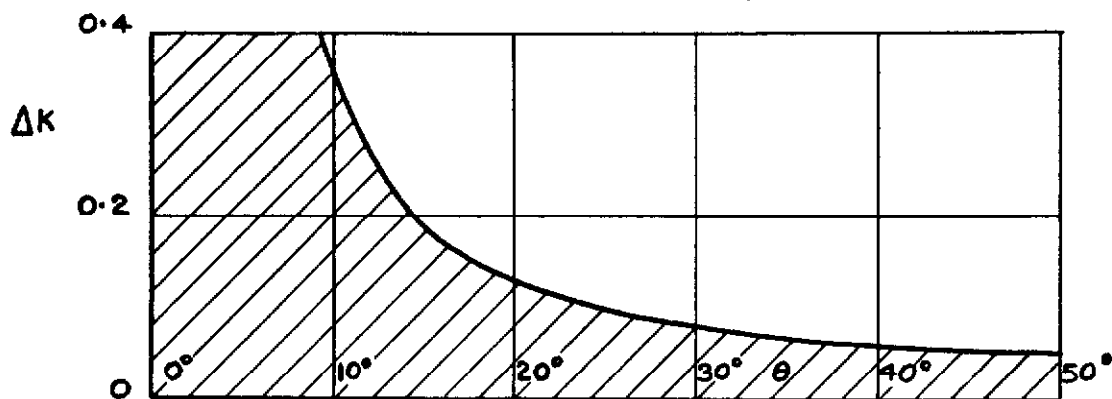
FIG. 4 30° CONE ($\epsilon = 15^\circ$) COMPARISON OF EXPERIMENTAL PRESSURE DISTRIBUTIONS WITH VALUES CALCULATED FROM NEWTONIAN THEORY. $M = 6.85$



(a) 25° TOTAL-ANGLE ($\epsilon = 12.5^\circ$)



(b) 30° TOTAL-ANGLE ($\epsilon = 15^\circ$)



(c) MAXIMUM EXPERIMENTAL ERROR

FIG. 5 (a - c) IMPACT COEFFICIENTS FOR 25° AND 30° CONES AT $M = 6.85$.

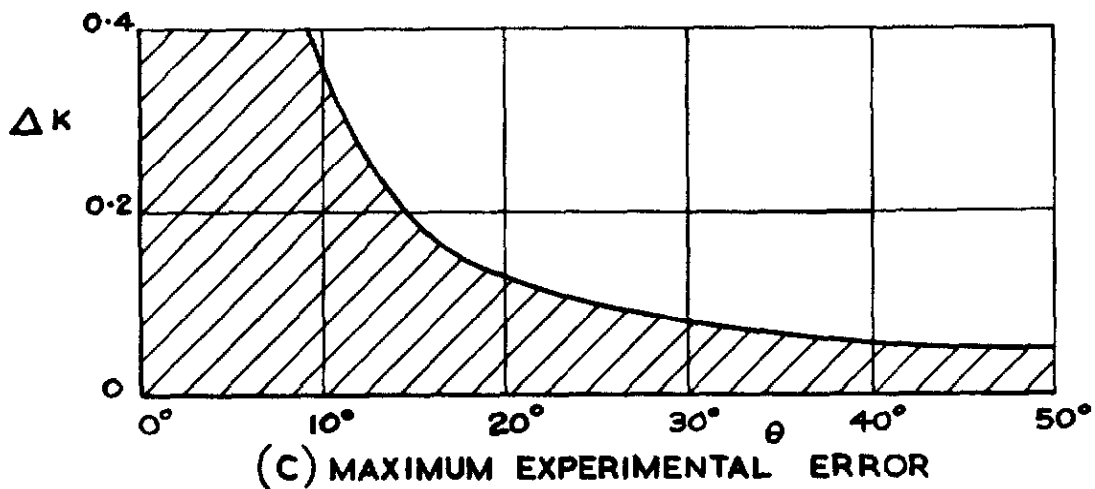
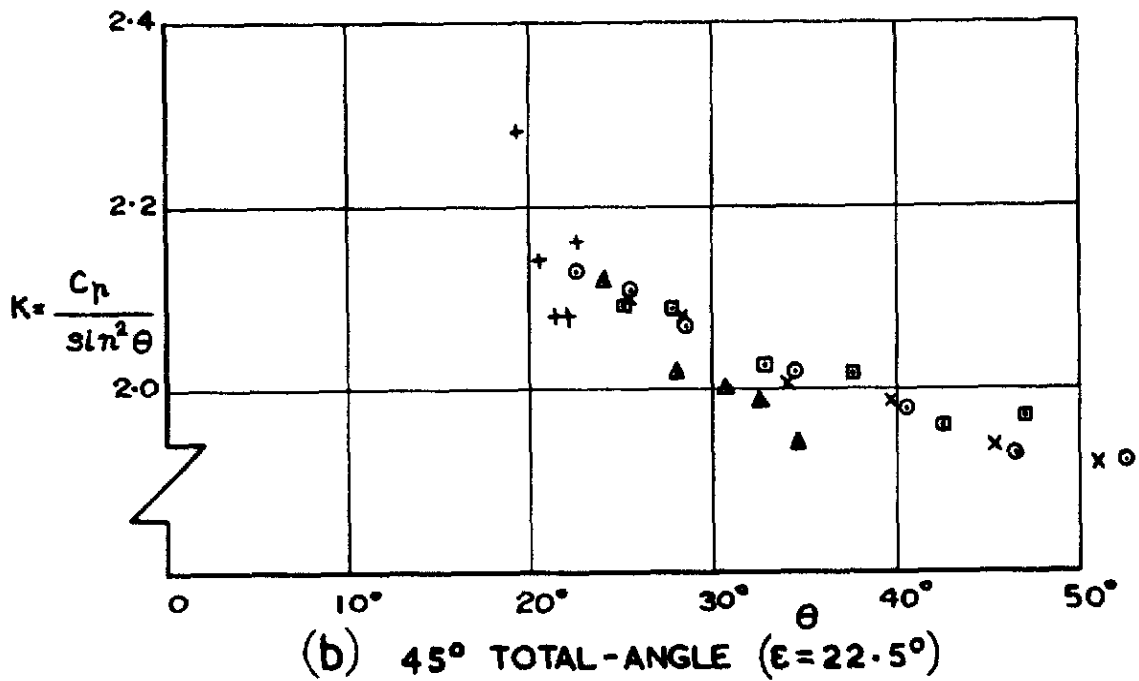
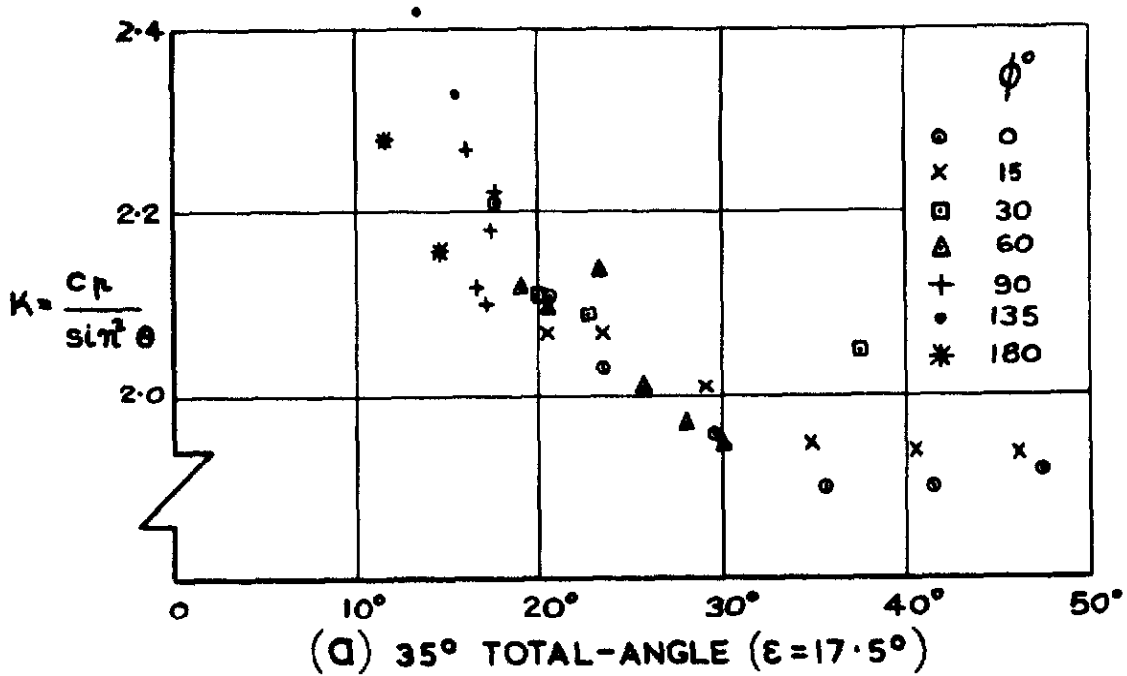
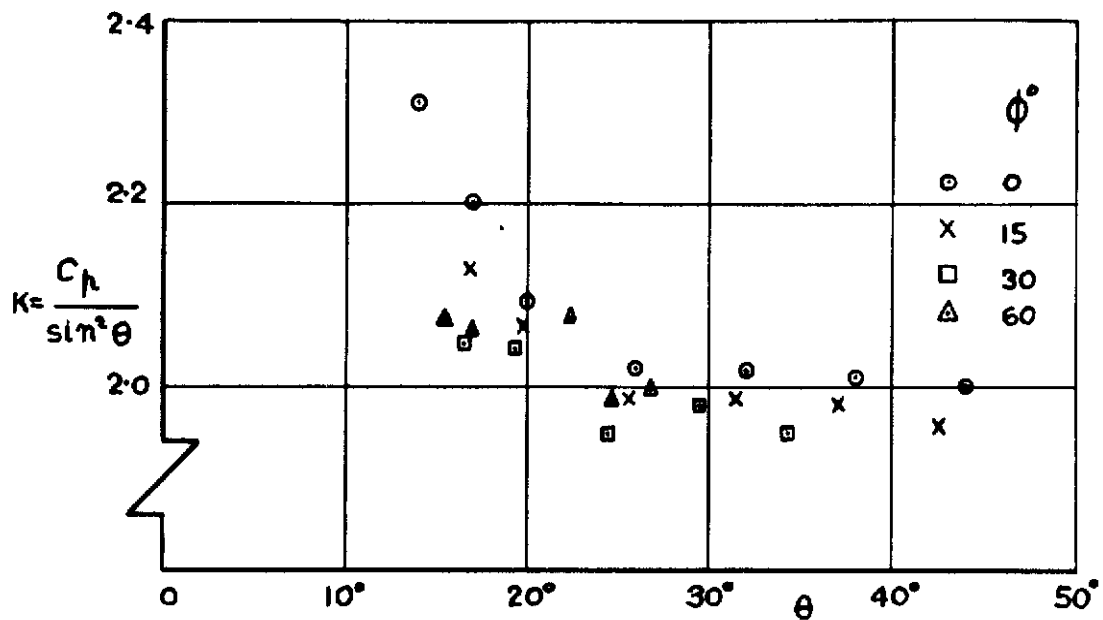
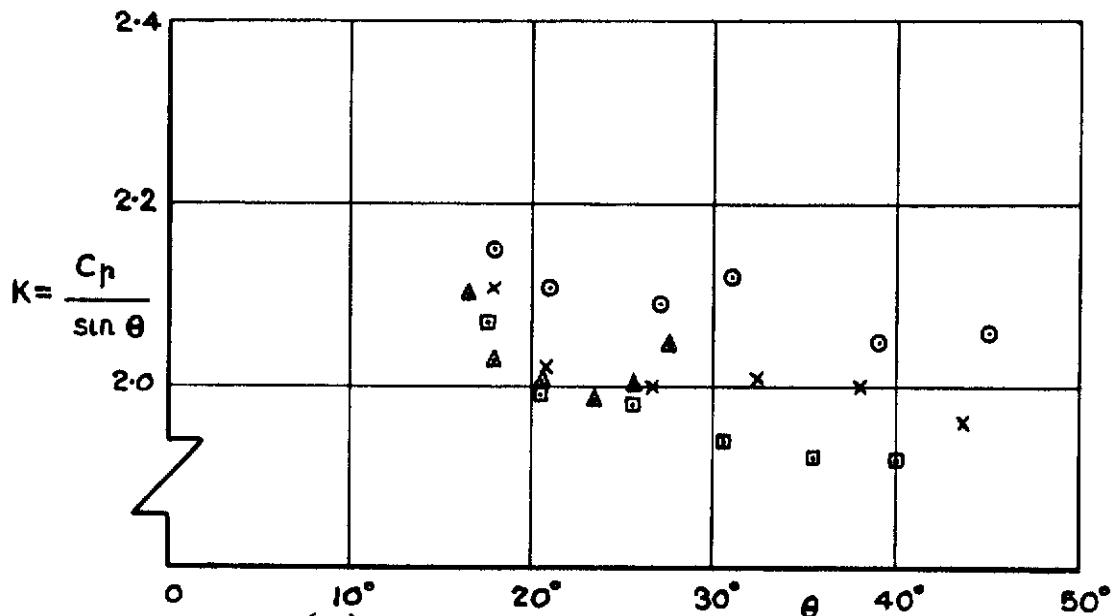


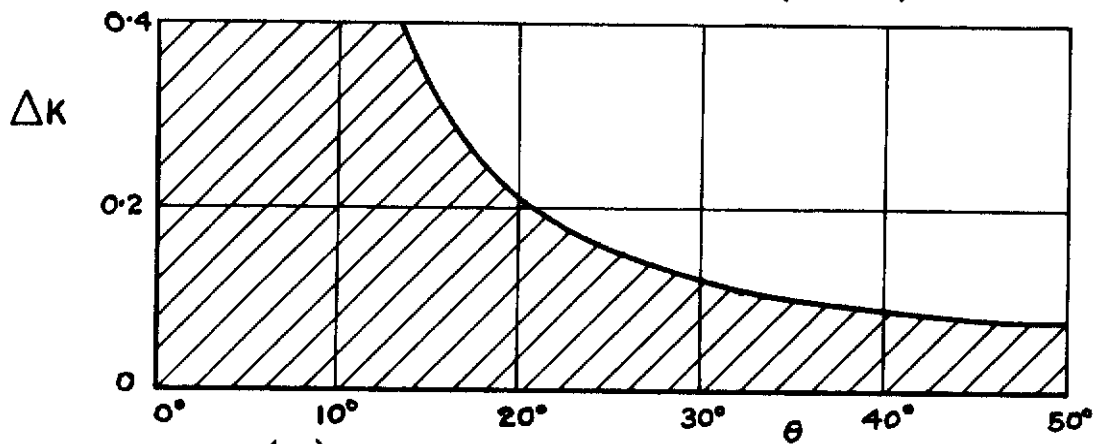
FIG. 6 (a - c) IMPACT COEFFICIENTS FOR 35° AND 45° CONES AT $M = 6.85$



(a) 28° TOTAL-ANGLE ($\epsilon = 14^\circ$)



(b) 30° TOTAL-ANGLE ($\epsilon = 15^\circ$)



(c) MAXIMUM EXPERIMENTAL ERROR

FIG. 7 (a - c) IMPACT COEFFICIENTS FOR 28° AND 30° CONES AT $M = 8.60$

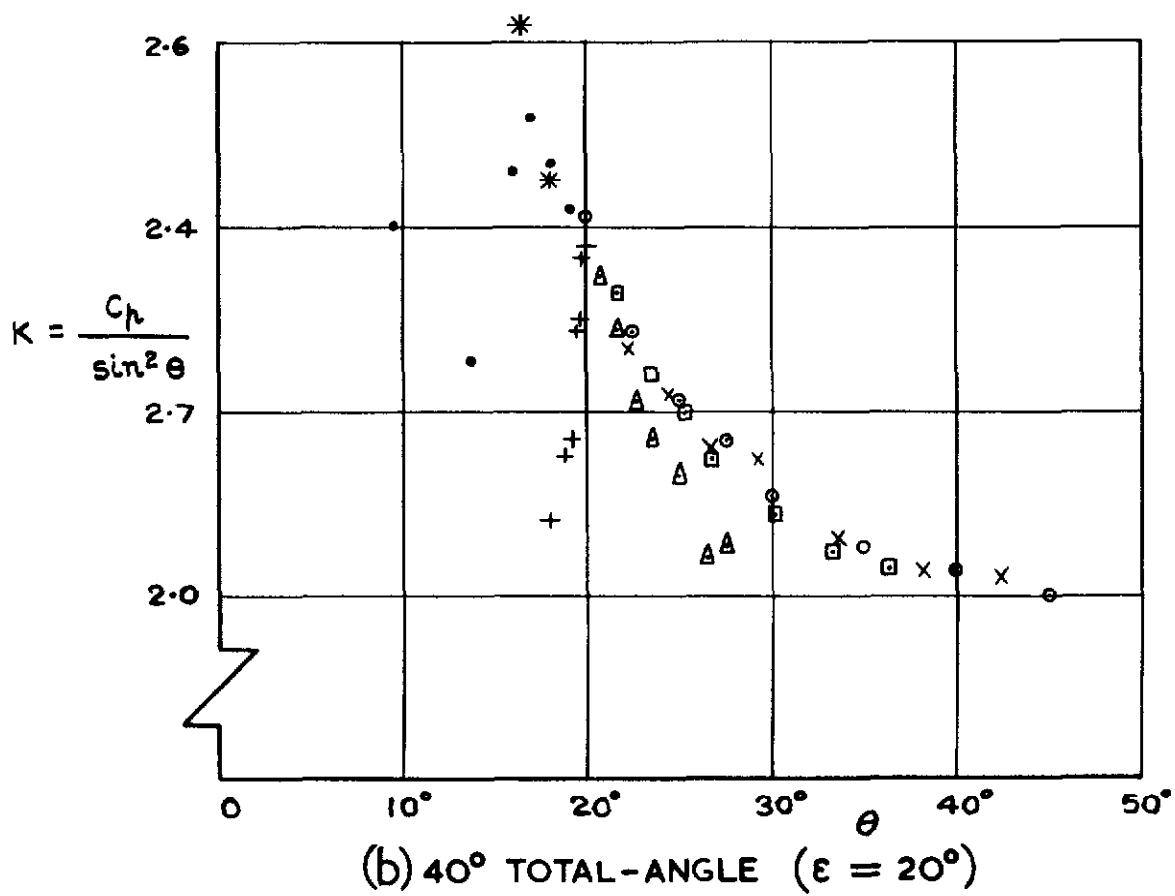
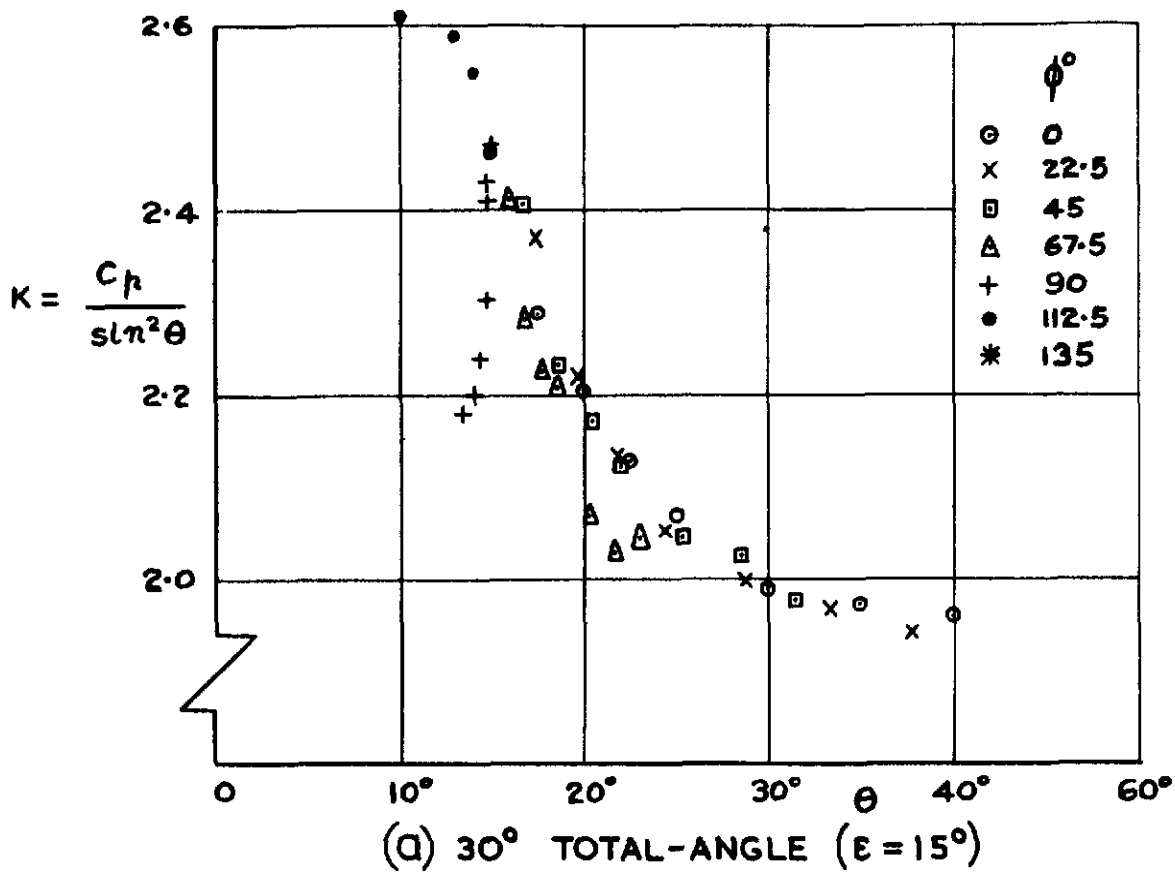
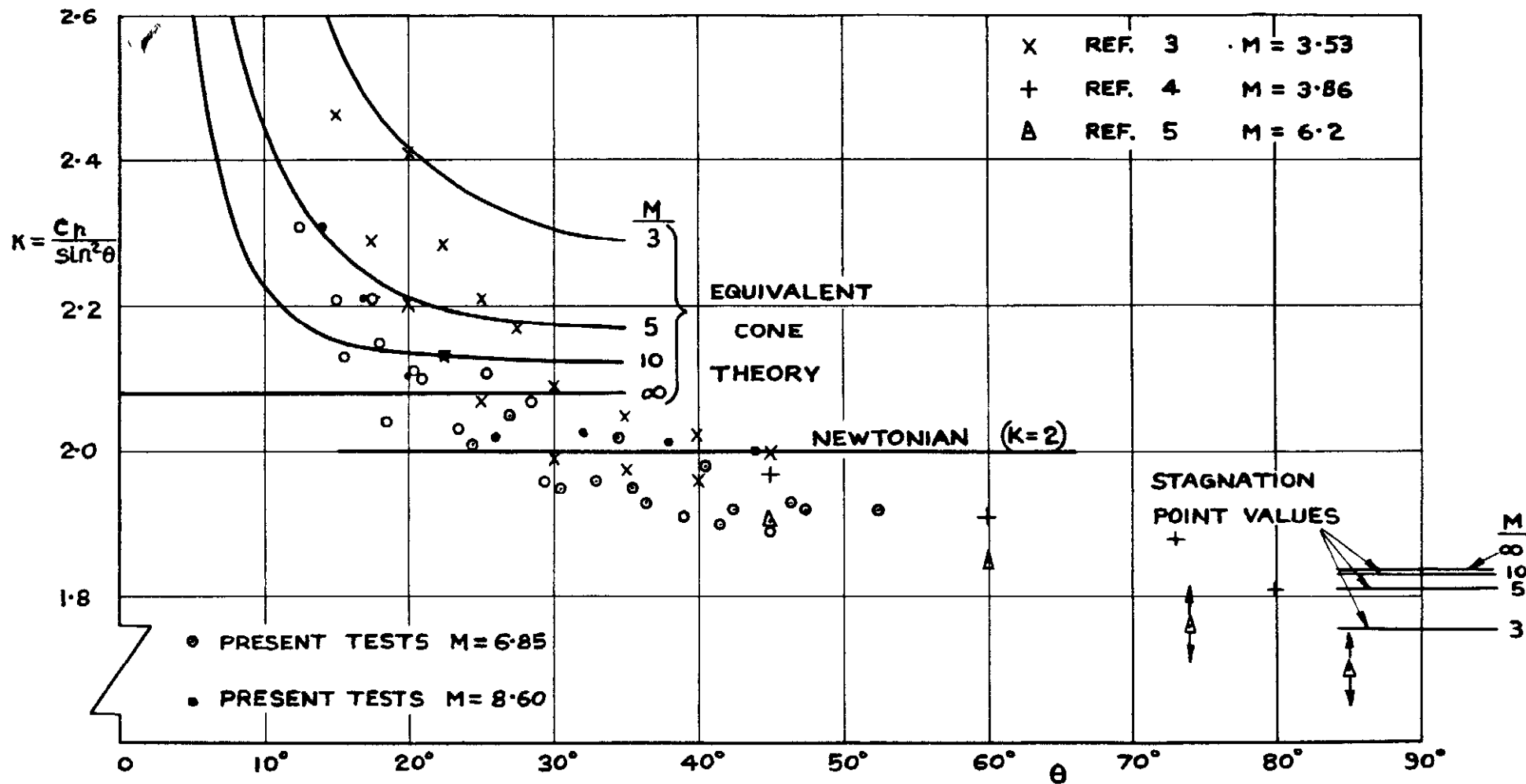


FIG. 8 (a & b) IMPACT COEFFICIENTS FOR 30° AND 40° CONES AT $M = 3.53$ (REF. 3).



(NOTE: TO AVOID CONFUSION, ONLY RESULTS OF MEASUREMENTS ON CONE WINDWARD GENERATORS ARE PLOTTED).

FIG.9 IMPACT COEFFICIENTS : SUMMARY OF AVAILABLE DATA $3.53 < M < 8.60$

A.R.C. C.P. No. 702

533.696.4 :
533.6.048.2 :
533.6.011.55

EXPERIMENTS AT HYPERSONIC SPEEDS ON CIRCULAR CONES AT INCIDENCE
Peckham, D.H. January 1963

Pressure distribution measurements on five circular cones with total apex-angles ranging from 25 to 45 degrees are described. The tests covered a range of angles of incidence from 0 to 30 degrees, at Mach numbers of 6.85 and 8.60. The extent to which various analytical and empirical theories predict the measured pressures is assessed.

A.R.C. C.P. No. 702

533.696.4 :
533.6.048.2 :
533.6.011.55

EXPERIMENTS AT HYPERSONIC SPEEDS ON CIRCULAR CONES AT INCIDENCE
Peckham, D.H. January 1963

Pressure distribution measurements on five circular cones with total apex-angles ranging from 25 to 45 degrees are described. The tests covered a range of angles of incidence from 0 to 30 degrees, at Mach numbers of 6.85 and 8.60. The extent to which various analytical and empirical theories predict the measured pressures is assessed.

A.R.C. C.P. No. 702

533.696.4 :
533.6.048.2 :
533.6.011.55

EXPERIMENTS AT HYPERSONIC SPEEDS ON CIRCULAR CONES AT INCIDENCE
Peckham, D.H. January 1963

Pressure distribution measurements on five circular cones with total apex-angles ranging from 25 to 45 degrees are described. The tests covered a range of angles of incidence from 0 to 30 degrees, at Mach numbers of 6.85 and 8.60. The extent to which various analytical and empirical theories predict the measured pressures is assessed.

© *Crown copyright 1965*

Printed and published by

HER MAJESTY'S STATIONERY OFFICE

To be purchased from

York House, Kingsway, London w c 2

423 Oxford Street, London w 1

13A Castle Street, Edinburgh 2

109 St Mary Street, Cardiff

39 King Street, Manchester 2

50 Fairfax Street, Bristol 1

35 Smallbrook, Ringway, Birmingham 5

80 Chichester Street, Belfast 1

or through any bookseller

Printed in England